Network RTK
– Concept and Performance

Ulrich Vollath, Herbert Landau, Xiaoming Chen
Trimble Terrasat GmbH, Hoehenkirchen 85635,Germany

Biography

Dr. Ulrich Vollath received a Ph.D. in Computer Science from the Munich University of Technology (TUM) in 1993. At Trimble Terrasat - where he is working on GPS algorithms since almost ten years - he is responsible for Algorithm Development team. His professional interest is focused on high-precision real-time kinematic positioning and reference station network processing.
Dr. Herbert Landau is Managing Director of Trimble Terrasat. He has many years of experience in GPS and has been involved in a large variety of GPS and GLONASS developments for high precision positioning systems and applications.
Dr. Xiaoming Chen is a software engineer at Trimble Terrasat. He holds a PhD in Geodesy from Wuhan Technical University of Surveying and Mapping.

Abstract

Traditionally, RTK positioning is limited due to the growth of the influence of systematic errors with the baseline length. Especially during periods of high ionospheric influences the maximum distance from the reference station allowing high productivity work for RTK positioning might become as low as 10 km or less.

The concept of virtual reference stations allows performing RTK positioning in reference station networks with distances of up to 40 km or more from the next reference station while providing the performance of short baseline positioning.

This paper gives a quantitative assessment of the data characteristics leading to the known rover performance improvements using data from various RTK/VRS networks from Asia, Europe, Australia and the U.S.A

Detail analyses explain the reduction of initialization times, improvement in position accuracy and increase in reliability seen in network RTK systems. It is demonstrated that network RTK does not only reduce the errors but also changes the error characteristics which lead to an additional performance increase in RTK positioning.

The important conclusion of the presented results is that once these changes in the error characteristics are fully understood and accounted for, more improvements in the performance of Network RTK applications can be expected.

Keywords: GPS; Network RTK; VRS; GPSNet

1. Introduction

The use of reference station networks has become the ubiquitous solution for high precision satellite positioning applications. The main systematic errors affecting the RTK rover performance are multipath, atmospheric and ephemeris errors. Whereas single base RTK is limited with respect to the distance between reference and rover the network RTK approach offers the possibility to increase the coverage area. It ideally leads to a situation in which the positioning error is independent of the rover position in the area of the network.

One technique proven in production systems for network RTK is the Virtual Reference Station (VRS) paradigm. It calculates network corrections for systematic errors based on real-time data from all reference stations, and simulating a local reference station for the user. Thus, the errors cancel out better than by using a more distant reference station.

One major effect from the application of VRS can be seen as a significant reduction of the temporal correlation of the ionospheric residual errors. Autocorrelation functions respective the autocorrelation time constants show this clearly. Improvements for multipath, tropospheric delay and ephemeris errors are achieved by VRS techniques, too. Taking the changes in the error characteristics into account, RTK systems could benefit even more from the use of reference station networks.

2. Virtual Reference Station (VRS) Concept

The Virtual Reference Station (VRS) concept is in commercial and research use since several years ([3], [4], [5]). The basic principles of Virtual Reference Stations operation are given in the following overview:

- Data from the reference station network is transferred to a computing center.
- The network data is used to compute models of ionospheric, tropospheric and orbit errors.

- The carrier phase ambiguities are fixed for the network baselines.
- The actual errors on the baselines are derived in centimeter accuracy using the fixed carrier phase observations.
- Linear or more sophisticated error models are used to predict the errors at the user location.
- A Virtual Reference Station (VRS) is created at the user location.
- The VRS data is transmitted to the user in standard formats (RTCM).

This concept is visualized in Figure 1. Real-time data from all base stations are used to predict the errors at the Rover location.

The user set-up in the field follows this procedure:

- The field receiver determines the user location with a navigation solution (no reference) or by DGPS (uncorrected data)
- The receiver dials into the computing center via mobile phone and is authenticated.
- The navigation solution is transferred to the computing center.
- The computing center immediately starts to send Virtual Reference Station data to the field user.

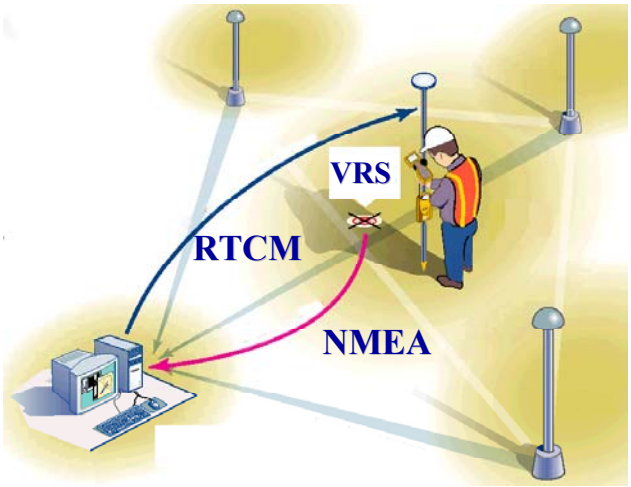

Figure 1: VRS field set-up procedure.

3. Performance Test Methodology

The significant effect of the VRS technique on productivity, reliability and precision of RTK positioning solutions has been observed many times ([6],[7]).

The aim of the investigations presented in this paper was to quantify the improvements of the measurement errors by distinguish the errors based on their statistical properties:

- Time correlated errors
- Uncorrelated (white noise type) errors
- Biases

3.1 Statistical Characterization

A first assumption taken here is that the time correlation can be defined by an exponential function. Tests have shown that this at least is a quite realistic assumption for a broad range of errors seen in GPS observables, as are ionospheric and tropospheric residuals and multipath.

Given the presence of uncorrelated (white noise) errors together with exponentially time correlated errors, the variance/covariance matrix of one time series for the double differences to one satellite is given by:

$$C = \begin{pmatrix} \sigma_c^2 + \sigma_u^2 & \cdots & \sigma_c^2 \cdot e^{-\frac{\Delta t}{t_c}} & \cdots \\ \vdots & \ddots & \vdots & \cdots \\ \sigma_c^2 \cdot e^{-\frac{\Delta t}{t_c}} & \cdots & \sigma_c^2 + \sigma_u^2 & \cdots \\ \vdots & \vdots & \vdots & \ddots \end{pmatrix}$$

Conversion to the correlation matrix yields:

$$R = \begin{pmatrix} 1 & \cdots & \frac{\sigma_c^2}{\sigma_c^2 + \sigma_u^2} \cdot e^{-\frac{\Delta t}{t_c}} & \cdots \\ \vdots & \ddots & \vdots & \cdots \\ \frac{\sigma_c^2}{\sigma_c^2 + \sigma_u^2} \cdot e^{-\frac{\Delta t}{t_c}} & \cdots & 1 & \cdots \\ \vdots & \vdots & \vdots & \ddots \end{pmatrix}$$

In Figure 2, the resulting autocorrelation function

$$R(\Delta t) = \begin{cases} 1, \Delta t = 0 \\ \frac{\sigma_u^2}{\sigma_u^2 + \sigma_c^2} \cdot e^{-\frac{\Delta t}{t_c}}, \Delta t > 0 \end{cases}$$

is rendered. In these formulas, the following notations were used:

- σ_c: correlated noise standard deviation
- σ_u: correlated noise standard deviation
- t_c: time constant

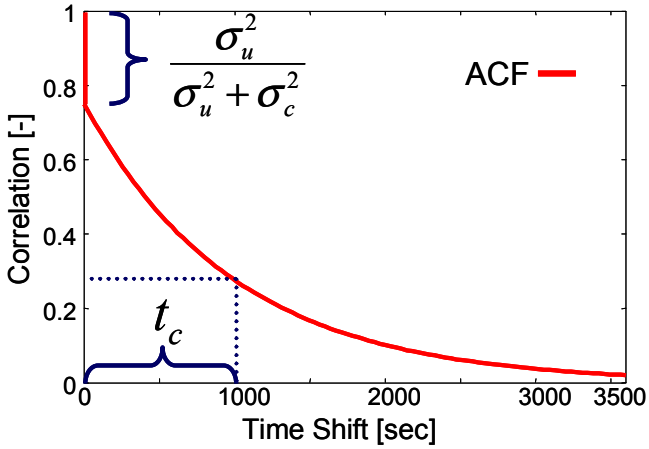

Figure 2: Auto-Correlation function

There is a characteristic jump at a time delay of 0 that reflects the ratio between the uncorrelated and the total error. The decay of the function is defined by the correlation time, where $R(t_c) = \frac{\sigma_u^2}{\sigma_u^2 + \sigma_c^2} \cdot e^{-1}$ is the characteristic correlation pointing at the correlation time.
To compute the correlated error, time constant and uncorrelated error, this auto-correlation function was not directly used. The reason is that a curve fit to the ACF using 2 parameters is only weakly determined. Instead, a new statistical evaluation was implemented that directly derives the three parameters and gives reasonably answer for short time spans of data. The importance of the separation of correlated and uncorrelated errors can be seen in Figure 2. If a simple exponential function $R(x) = e^{-\frac{\Delta t}{t_c}}$ is fitted to the ACF, the time constant will be estimated much too low.

In addition, the mean value for every residual time series was computed to reflect the systematic errors present in the data.

3.2 Motivation

One question that could be posed here is why such an effort is necessary. In Figure 3 the difference between uncorrelated errors and time correlated errors can easily be seen for the formal evolution of the standard deviations of an estimate.

All values are relative to the standard deviation of a single measurement. The uncorrelated time series errors reduce by far faster than for the correlated data. This has two consequences. The reduction of the time constant is crucial for fast convergence. This affects the time until ambiguities can be resolved (time-to-fix) as well as the time needed to acquire a given precision for a position computation (time-to-precision). Also, knowing the time constant, better predictions can be done for the accuracy reached after a given time of data accumulation. If the knowledge of the time correlation is limited, either the expected errors are too optimistic leading to a poor reliability or too pessimistic resulting in a poor availability and productivity.

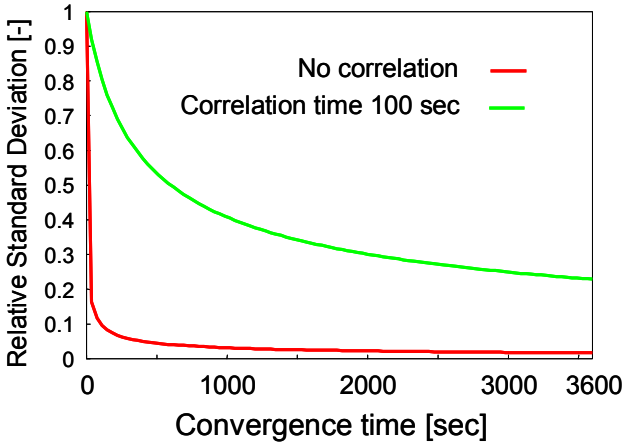

Figure 3: Convergence for white and correlated noise

3.3 Observation Selection

For every data set, the ambiguities were solved in post-processing. Then, the double-difference residuals were created using the precise position of the respective receiver antenna for the following phase combinations:
Ionospheric carrier phase combination, a.k.a. geometry-free combination:

$$\phi_{iono} = (\lambda_{L1} \cdot \phi_{L1} - \lambda_{L2} \cdot \phi_{L2}) \cdot \frac{\lambda_{L1}^2}{\lambda_{L2}^2 - \lambda_{L1}^2}$$

Geometric carrier phase combination ([1]):

$$\phi_{geo} = a \cdot \lambda_{L1} \cdot \phi_{L1} + (1-a) \cdot \lambda_{L2} \cdot \phi_{L2}$$

The geometric ranges between satellites and receivers and an a priori tropospheric model (modified Hopfield, [1]) were removed from the geometric residuals in the common way.

4. Error Characteristics Analysis

4.1 Test Networks

Six networks (see Figure 4) operated with Trimble GPSNet software were used for the analyses.

For every network, one reference receiver was taken out of the network processing and used as the user receiver (rover).

The following enumeration gives location, time of data collection and the distance of the rover station to the nearest reference station.

1. Queensland, Australia, February 2001, 31 km
2. Kanto, Japan, January 2002, 26 km
3. Thueringen, Germany, August 2002, 19 km
4. Bavaria, Germany, May 2002, 31 km
5. California, U.S.A., November 2001, 25 km
6. North Carolina, U.S.A., September 2002, 27 km

For every network, 24 hours of data were used to include day- and night-time.

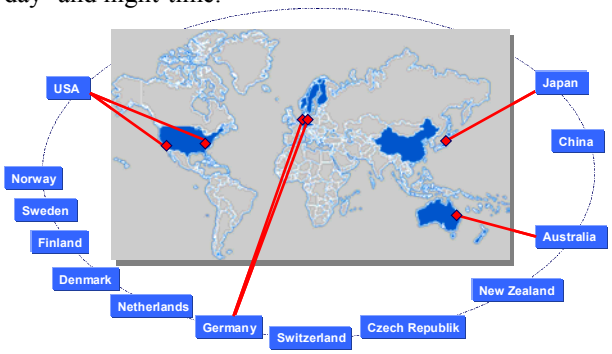

Figure 4: GPSNet VRS installations used for the tests

The data of the network stations excluding the rover station was processed using a post-processing version of the real-time VRS software GPSNet. Instead of the usual dial-in functionality to generate VRS RTCM data, the virtual

reference station data was generated using the same algorithms but written into a post-processing file format.

Then a standard GPS post-processing software (Trimble Total Control) was used to determine the fixed ambiguities for the long baseline (rover to nearest reference station) and the VRS baseline.

Using these ambiguities and precise coordinates for the stations involved, the residuals were derived in the way described above. For every time series, i.e. every satellite double difference residuals series the auto-correlation analysis was performed.

4.2 Analysis Results

A typical example of the error reduction by VRS processing is shown in Figure 5 for the California network.

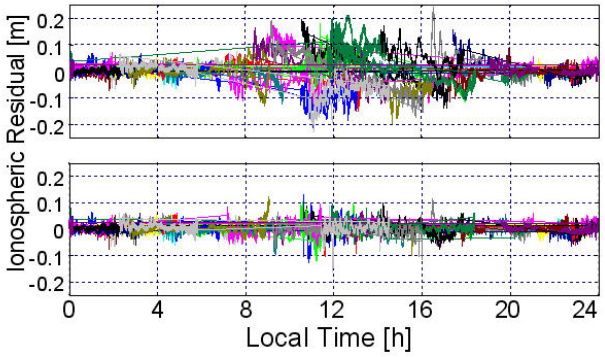

Figure 5: Ionospheric residuals without and with VRS

It can be clearly seen that the raw data (upper graph) includes a substantial increase of the ionospheric residuals during daytime. This is very much mitigated in the VRS data (lower graph). Though this is obvious, the detailed statistical analyses for all data lead to insights not available from a simple look at the data.

Table 1 (located at the end of this paper) presents a compilation of the analysis results. Correlation time t_{cor}, bias, correlated error standard deviation σ_{cor} and uncorrelated error standard deviation σ_{unc} are given for ionospheric and geometric residuals separately. For every network, the raw data residuals, VRS residuals and the improvement factor between both are given. The last row gives the mean improvement factors over all networks.

The improvements are visualized in the following figures. They give bars for raw ionospheric residuals, VRS ionospheric residuals, raw geometric residuals and VRS geometric residuals respective.

The results are given for all networks separately and are labeled as follows:

- AUS: Australia network
- JP: Japan Network
- GER1: Thueringen, Germany
- GER2, Bavaria, Germany
- CA: California, U.S.A
- N.C.: North Carolina, U.S.A.

Figure 6 shows mainly the effects that were studied in the past, i.e. the improvements of the correlated errors as the main contribution.

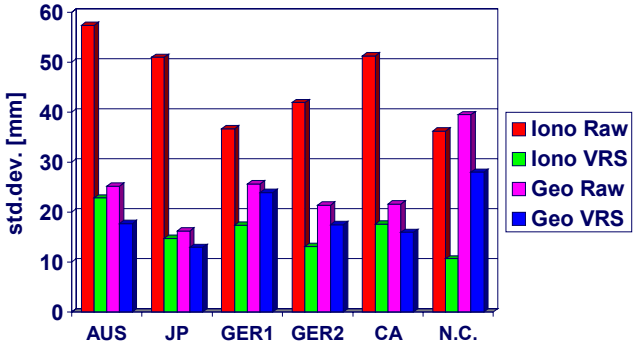

Figure 6: Correlated errors

Nevertheless, this information is not complete without a look at Figure 7 showing the time constants for the time-correlated errors. Especially for the ionosphere, a very high improvement can be seen. For the geometric error, the improvements are marginal. This should be subject to further studies.

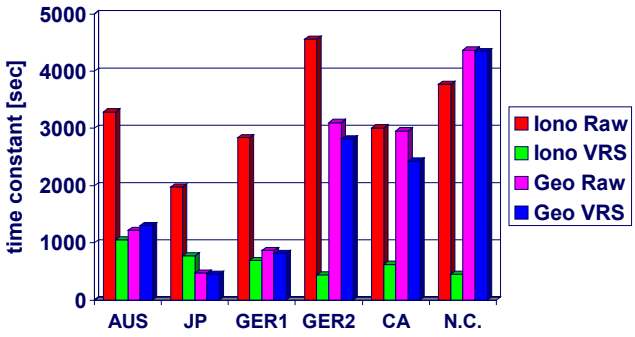

Figure 7: Time constants

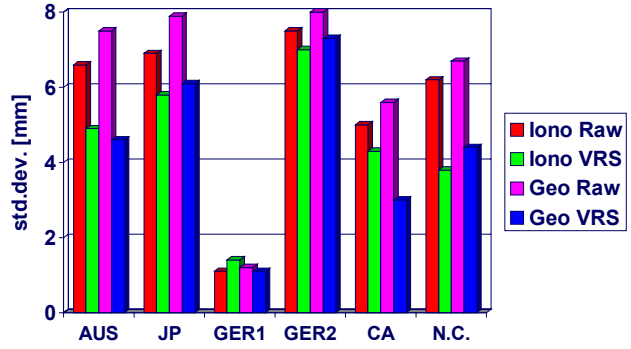

Figure 8: Uncorrelated errors

The "noise part" of the errors is shown in Figure 8. The improvements are in the tens of percent range. One reason is

that only the reference side can be influenced, while mitigation for the rover side is not possible. This applies to multipath which is not separately studies in this paper, too. Still this is an advantage in kinematic applications where averaging in the position domain is not feasible.

One important factor for the data quality is the presence of biases in the measurements. They lead to systematic errors in the positions computed and can also impact the time-to-fix. Figure 9 displays the biases derived for the data sets.

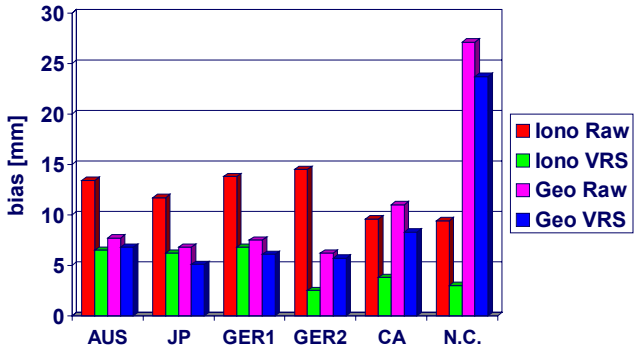

Figure 9:Biases

The following figures summarize the improvement factors for all the information shown before.

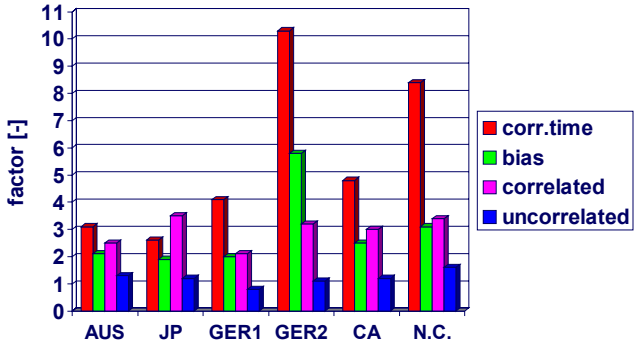

Figure 10: Ionosphere improvements

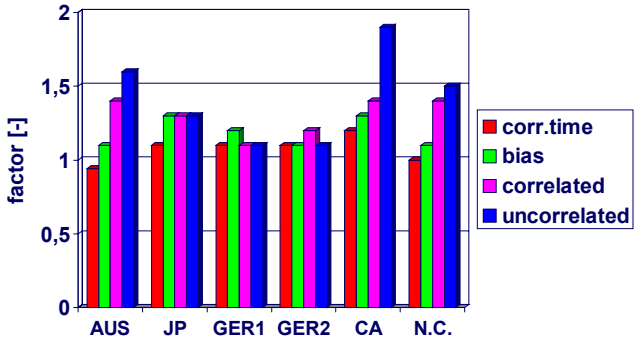

Figure 11: Geometric residual improvements

The improvements achieved when using VRS were the initial motivation for this study. Nevertheless, an example follows to visualize one improvement the VRS user can expect.

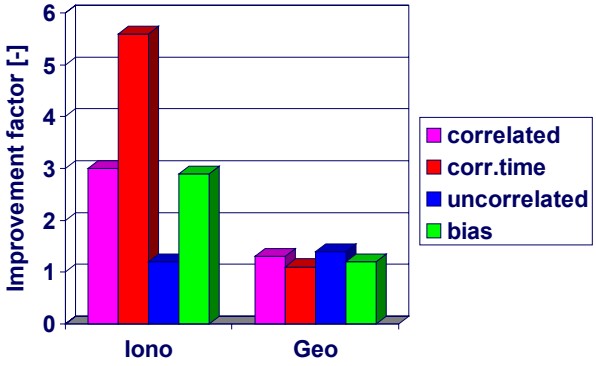

Figure 12: Mean improvements

In Figure 13 an example is given for the effect of the improvement of the geometric residuals on the positioning performance, i.e. the performance indicator the user is finally interested in.

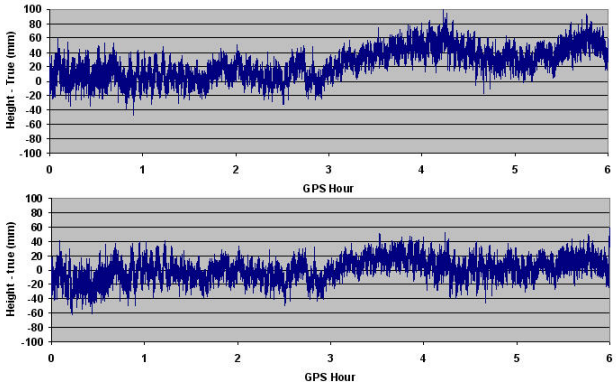

Figure 13: Height performance without and with VRS

While the raw data (upper graph) shows systematic effects up to 8 cm in the height component, this could be reduced to 4 cm by using VRS. Additional investigations proved that the origin of this height error is a strong tropospheric error in the data.

5. Real-time Performance Test

5.1 Test Description

As a test network, a part around Munich, Germany of the BLVA network of the land surveying authorities in Bavaria has been used. This test-bed is continuously operated for GPSnet software testing and development. The network consists of 7 stations, each station has a dual-frequency GPS receiver and is permanently connected to the Trimble Terrasat office via leased data lines. The network configuration is shown in Figure 14 including the inter-station baseline lengths.

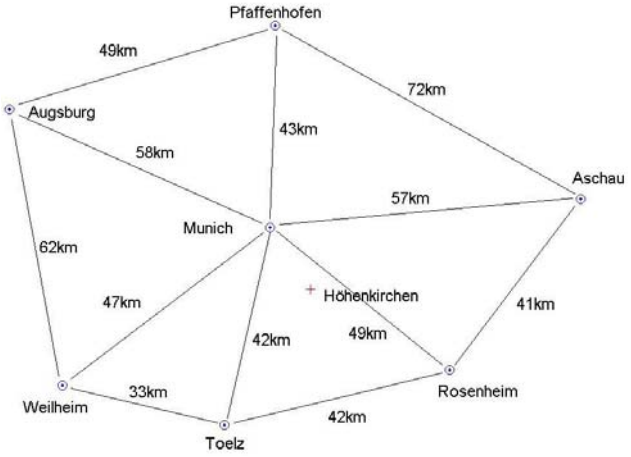

Figure 14: Munich test network used for RTK evaluation in single-baseline and broadcast network modes.

The Trimble Network RTK software [Trimble, 2002] can be operated in either a VRS or Broadcast mode. The broadcast mode was used for the tests described below.

Four concurrent tests were run over a 40-hour period to evaluate the performance of RTK in single-baseline and network modes. Four Trimble 5700 receivers were connected to the same antenna at the Trimble Terrasat office at Höhenkirchen. Standard single-baseline data was fed from Munich and Toelz into two 5700 receivers, thus giving rise to 16km and 32km baselines, respectively. Network corrections were input to the other two 5700 receivers at Höhenkirchen. One set of corrections was derived from the entire network, while the second correction stream was created without the nearest network station - Munich.

5.2 Test Results

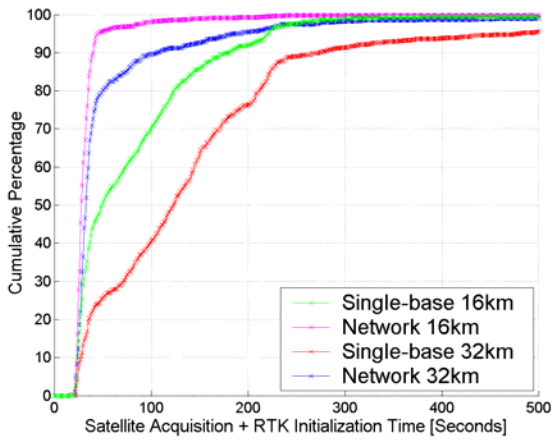

Figure 15: Height performance without and with VRS Cumulative probability of ambiguity resolution for single-base and network modes over 16km and 32km baselines.

Figure 15 illustrates the cumulative time-to-initialise for the 4 different 5700 receivers. The results of network corrected data provide very noticeable benefits for the time-to-initialise statistics. The 16km baseline with network corrections exhibits the sharpest elbow in figure 15. In other words, the majority of initialisations occur within a short period of time. The network-corrected 16km baseline results are comparable to those regularly achieved with single-baseline RTK on lines less than 10km where ionospheric biases are typically small. The 32km baseline with network corrections has the next-best performance. The single-base RTK results for the 16 and 32km lines exhibit the worst initialisation times.

6. Summary

The VRS technique has proven the potential to reduce several main error sources in GPS positioning. For the ionosphere impact, most error characteristics have an average improvement factor between 2 and 10. It should be noted here that these improvements would be even higher if day data only would be analyzed, one proposal for continuing this study. Uncorrelated noise is reduced less, but still in a way that can be significant for kinematic applications.

Geometric errors, and, as the broadcast orbits are very good since a while, mainly tropospheric residuals are also reduced up to 40 % leading to improved positioning. Here a still a potential for further improvements to go to the limits of what can be achieved for a local effect like tropospheric errors.

The most surprising result was the presence of very high correlation times in both the ionospheric and the geometric errors in the range of 1 hour. The consequence is that simple averaging techniques are by far not sufficient for productive RTK positioning as here the user expects a time-to-fix in the tens of seconds to few minutes.

There are two coexisting solutions for this problem. The first is to implement more information about the errors into the RTK system algorithms, i.e. physical modeling of the ionosphere, tropospheric scaling techniques, etc. The other method is application of the VRS technique. As has been demonstrated, especially for the ionospheric errors the magnitude, but even more the correlation times of the errors are significantly reduced. This provides a new insight about how VRS-assisted RTK works.

7. Acknowledgement

The authors thank the networks used for availability of the data used. They helped to improve understanding of VRS and future improvements of this technique.

8. References

[1] Goad, C.C. and L. Goodman, 1974, A modified Hopfield tropospheric correction model, Presented at the American Geophysical Union Fall Annual Meeting, San Francisco, December 12-17.

[2] Sjöberg, L: The Best Linear Combination of L1 and L2 Frequency Observables in the Application of Transit/Doppler and GPS, manuscripta Geodetica 15 (1990), p. 17-11.

[3] Talbot, N., Lu, G., Allison, T. and Vollath, U.: Broadcast Network RTK – Transmission Standards and Results, Accepted for Proceedings of the ION GPS 2002, Sep. 2002

[4] Trimble, 2002, Trimble Virtual Reference Station (VRS), product brochure, Sunnyvale, California, 8 pages.(available at: http://www.trimble.com/vrs.html)

[5] Vollath, U., Buecherl, A., Landau, H. Pagels, C., Wagner, B.: Multi-Base RTK using Virtual Reference Stations, Proceedings of ION GPS 2000, Salt Lake City, Utah, September 19-22.

[6] Vollath, U., A. Buecherl, H. Landau, C. Pagels, B. Wagner, 2000a, Multi-Base RTK using Virtual Reference Stations, Proceedings of the ION-GPS 2000, Salt Lake City, Utah

[7] Vollath, U., A. Buecherl, H. Landau, C. Pagels, 2001, Long-Range RTK Positioning Using Virtual Reference Stations, KIS-2001.

Table 1: Overview of all test results

Data Set		Ionospheric Residuals				Geometric Residuals			
		t_{cor} [sec]	bias [mm]	σ_{cor} [mm]	σ_{unc} [mm]	t_{cor} [sec]	bias [mm]	σ_{cor} [mm]	σ_{unc} [mm]
Australia	31 km	3290	13.4	57.4	6.6	1221	7.7	25.2	7.5
	VRS	1052	6.5	22.8	4.9	1304	6.8	17.7	4.6
	f_{impr}	3.1	2.1	2.5	1.3	0.94	1.1	1.4	1.6
Japan	26 km	1977	11.7	51.0	6.9	472	6.8	16.2	7.9
	VRS	771	6.2	14.7	5.8	448	5.1	12.9	6.1
	f_{impr}	2.6	1.9	3.5	1.2	1.1	1.3	1.3	1.3
Germany 1	19 km	2835	13.8	36.7	1.1	868	7.5	25.6	1.2
	VRS	693	6.8	17.3	1.4	815	6.1	23.9	1.1
	f_{impr}	4.1	2.0	2.1	0.8	1.1	1.2	1.1	1.1
Germany 2	31 km	4557	14.5	41.9	7.5	3103	6.2	21.4	8.0
	VRS	442	2.5	13.1	7.0	2818	5.7	17.5	7.3
	f_{impr}	10.3	5.8	3.2	1.1	1.1	1.1	1.2	1.1
California	25 km	3008	9.6	53.1	5.0	2958	11.0	21.6	5.6
	VRS	623	3.8	17.6	4.3	2426	8.3	15.9	3.0
	f_{impr}	4.8	2.5	3.0	1.2	1.2	1.3	1.4	1.9
N.Carolina	27 km	3772	9.4	36.2	6.2	4367	27.1	39.5	6.7
	VRS	450	3.0	10.6	3.8	4343	23.7	28.0	4.4
	f_{impr}	8.4	3.1	3.4	1.6	1.0	1.1	1.4	1.5
Mean	f_{impr}	5.6	2.9	3.0	1.2	1.1	1.2	1.3	1.4